Thermochromism in Yttrium Iron Garnet Compounds

ARTICLE *in* INORGANIC CHEMISTRY · NOVEMBER 2014

Impact Factor: 4.76 · DOI: 10.1021/ic501708b · Source: PubMed

10 AUTHORS, INCLUDING:

Hélène Serier-Brault
University of Nantes
27 PUBLICATIONS **224** CITATIONS
SEE PROFILE

Jean Waku
SEB Group
3 PUBLICATIONS **3** CITATIONS
SEE PROFILE

Inorganic Chemistry

Article

pubs.acs.org/IC

Thermochromism in Yttrium Iron Garnet Compounds

Hélène Serier-Brault,*[,†] Lucile Thibault,[†] Magalie Legrain,[†] Philippe Deniard,[†] Xavier Rocquefelte,[†] Philippe Leone,[†] Jean-Luc Perillon,[‡] Stéphanie Le Bris,[‡] Jean Waku,[‡] and Stéphane Jobic*[,†]

[†]Institut des Matériaux Jean Rouxel, Université de Nantes, CNRS, 2 rue de la Houssinière, BP 32229, 44322 Nantes cedex, France

[‡]Tefal SA, Chemin des Granges, 74150 Rumilly, France

ABSTRACT: Polycrystalline yttrium iron garnet ($Y_3Fe_5O_{12}$, hereafter labeled YIG) has been synthesized by solid-state reaction, characterized by X-ray diffraction, Mössbauer spectroscopy, and UV−vis-NIR diffuse reflectance spectroscopy, and its optical properties from room temperature (RT) to 300 °C are discussed. Namely, its greenish color at RT is assigned to an $O^{2-} \rightarrow Fe^{3+}$ ligand-to-metal charge transfer at 2.57 eV coupled with d−d transitions peaking at 1.35 and 2.04 eV. When the temperature is raised, YIG displays a marked thermochromic effect; i.e., the color changes continuously from greenish to brownish, which offers opportunities for potential application as a temperature indicator for everyday uses. The origin of the observed thermochromism is assigned to a gradual red shift of the ligand-to-metal charge transfer with temperature while the positioning in energy of the d−d transitions is almost unaltered. Attempts to achieve more saturated colors via doping (e.g., Al^{3+}, Ga^{3+}, Mn^{3+}, ...) remained unsuccessful except for chromium. Indeed, $Y_3Fe_5O_{12}$:Cr samples exhibit at RT the same color than the undoped garnet at 200 °C. The introduction of Cr^{3+} ions strongly impacts the color of the $Y_3Fe_5O_{12}$ parent either by an inductive effect or, more probably, by a direct effect on the electronic structure of the undoped material with formation of a midgap state.

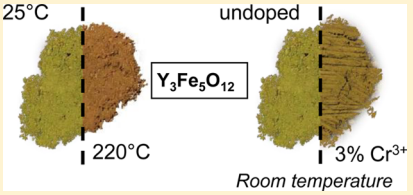

1. INTRODUCTION

Thermochromic inorganic materials change color with a temperature variation (heating or cooling) and offer potentialities for temperature indicators[1,2] in different kinds of devices, such as temperature sensors for safety (kitchen tools, hot plates, fridges, ...), laser marking, or warning signals. Color change can be brutal or continuous, reversible or irreversible according to the involved mechanism. An irreversible color change is mainly associated with a chemical transformation, i.e., a decarbonation or a dehydratation reaction,[3] for instance. A material with such an effect has restricted applications and is mainly used for the monitoring of temperature-sensitive products. In contrast, materials with reversible thermochromism can give rise to many applications in daily living. Each application requests then specific characteristics in terms of color, transition temperature range, color contrast, or cyclability. For obvious reasons, materials with saturated hues in the low- and high-temperature states should be privileged for an optimal visual rendering and industrial applications.

For oxides, reversible thermochromism may originate from a gradual reduction of the band gap[4] with a temperature increase (red shift) as commonly observed for semiconductors, a change in the ligand field around the chromophor, or a crystallographic phase transition.[5−9] The major restriction in the use of semiconductors lies in their limited choice of colors (namely, white, yellow, orange, red, or black) and the difficulty to assign an accurate temperature to a given hue by the naked eye due to a continuous color change in the chromatic coefficients with temperature. The d−d transitions can lead to interesting colors in crystal with sometimes thermochromic effects (e.g., Cr^{3+}-doped Al_2O_3), but without high color strength.[1,2] Materials that undergo a phase transition (namely, first-order transition) may display very pronounced color contrast in relation to change in coordination of chemical elements, for instance. Unfortunately, the volume variation at the transition may reduce considerably their cyclability[8] if too large. In that domain, metal−insulator transitions (e.g., VO_2[10]) have received much attention due to their ability to reflect or to absorb IR wavelengths and control the energy exchange through windowpanes in buildings. Nevertheless, no color change is observed in the visible range when the material shifts from metallic to semiconductor.

To have access to a large panel of colors (i.e., colors others than those generated by valence band (VB)−conduction band (CB) transition), transition elements have to be present to take advantage of d−d transitions in the visible region. In first approximation, the positioning of these d−d transitions is much less dependent on temperature than ligand-to-metal transfer or VB−CB transitions. Thus, a solution to obtain a large variety of colored materials with thermochromic properties may consist in mixing a semiconductor material with a d−d transition-based compound. In that case, it is possible to fully design various reversible thermochromic effects with a control of the transition temperature, a control of the blend hues with T, and a good cyclability. This mixing rule was already discussed in the literature for Bi_2O_3−$CoAl_2O_4$, Bi_2O_3−$LiCoPO_4$, and V_2O_5−Cr_2O_3 blends.[11] However, this technique has some shortcomings especially concerning the color which is not saturated enough because of the subtractive synthesis principle of colors.

The ideal way to get a reversible and robust (high cyclability) thermochromic material will be to get a pigment with a color originating from the intrinsic mixing rule (charge transfer

Received: July 17, 2014
Published: November 10, 2014

   dx.doi.org/10.1021/ic501708b | Inorg. Chem. 2014, 53, 12378−12383

located in the visible range together with d−d transitions). Herein, we report the investigation of a well-known compound, the yttrium iron garnet ($Y_3Fe_5O_{12}$, hereafter labeled YIG) with a greenish color at room temperature. For the first time, thermochromic properties of YIG are measured and displayed. Unfortunately, the colors of YIG are far from being saturated. This prompted us to investigate the impact of the insertion of dopant in the $Y_3Fe_5O_{12}$ host lattice on the color. Several dopants were tried (e.g., Al^{3+}, Ga^{3+}, Mn^{3+}, ...), but only chromium ions get an effect on the color of the parent material.

2. EXPERIMENTAL SECTION

Conventional high-temperature solid-state reactions were performed to synthesize $Y_3Fe_5O_{12}$ and $Y_3Fe_{5-x}Cr_xO_{12}$ compounds. The constituent oxides Y_2O_3 (Alfa Aesar, 99.9%), Fe_2O_3 (Alfa Aesar, 99.945%, <5 μm powder), and Cr_2O_3 (Alfa Aesar, 99.997%) were used as starting materials. The raw materials were weighed in stoichiometric proportions and ball-milled with ethanol in a Fritsch Pulverisette 7. Then, the blends were dried at 100 °C and annealed at 1350 °C in air during 6 h to finally lead to a greenish powder. As-synthesized powders were ball-milled 10 min before X-ray, Mössbauer, and optical characterizations.

Phase purity and crystal structure were examined by powder X-ray diffraction (PXRD) analysis with a Bruker AXS D8 advanced automatic diffractometer with Cu K-L_3 radiation (germanium monochromator) operating at 40 kV and 40 mA. The XRD patterns were collected in the 10−90° 2θ with a 0.02° step range. The structures were refined with the full-matrix least-squares technique using the Jana2006 program.[12] The errors bars on all parameters were calculated as three times the Berar's[13] coefficient multiplied by the standard deviation. To record data as a function of temperature, a Brüker "D8 Advance" powder diffractometer equipped with an Anton Paar HTK 1200 N high-temperature attachment was used. Data were collected in the Bragg−Brentano geometry with a Cu-anode X-ray source ($Cu_{K\text{-}L2}$, $Cu_{K\text{-}L3}$) operated at 40 kV and 40 mA. A 1-D position-sensitive detector ("Vantec" detector) with an active area restricted to 3° 2θ was employed to improve the angular resolution of XRD patterns. The Cu Kβ radiation was filtered by means of a Ni foil.

Room-temperature UV−visible diffuse reflectance spectra were recorded on a PerkinElmer Lambda 1050 for each finely ground sample. For room-temperature spectra, the spectrophotometer was equipped with an integrating sphere coated with Spectralon, a highly reflecting fluoropolymer. For measurements versus temperature, the spectrometer was fit with a praying mantis accessory. All spectra were recorded between 200 and 1200 nm with a 1 nm step. The absorption (α/S) values were calculated from the reflectance using the Kubelka−Munk transformation: $\alpha/S = (1 - R)^2/2R$, where R is the reflectance at the given wavelength, α is the absorption coefficient, and S is the scattering coefficient. The S value is supposed to be particle size independent since grains size is larger than a few micrometers. The CIE 1976 color parameters have been determined from optical measurements with D65 as illuminant and a observer at 2°.

Mössbauer spectra were obtained with a constant acceleration automatic folding Elscint-type spectrometer using a room-temperature ^{57}Co(Rh) source in transmission geometry and a triangular reference signal. α-Fe was used as reference. The spectra were computed with a least-squares routine using Lorentzian lines. To obtain an acceptable accuracy, a velocity scale of 11.78 mm/s was used at room temperature.

3. RESULTS AND DISCUSSION

3.1. Synthesis and Structure Characterization of $Y_3Fe_5O_{12}$. Yttrium iron garnet (YIG) belongs to the garnet family with the chemical composition $\{Y_3\}[Fe_2^{3+}]_a(Fe_3^{3+})_dO_{12}$ and crystallizes in the space group $Ia\bar{3}d$ (SG No. 230).[14] In this structure, yttrium ions occupy a dodecahedral site (24c), where a and d represent the octahedral (Wyckoff position 16a) and tetrahedral (Wyckoff position 24d) sites of Fe^{3+}ions, respectively. Each octahedron (tetrahedron) is linked to six (four) others via corner-sharing tetrahedra[14,15] (octahedra) to provide a three-dimensional structure. The YIG structure is mainly described in the literature in the cubic space group $Ia\bar{3}d$, but Rodic et al.[16] used the trigonal space group $R\bar{3}$ (SG No. 148) to account for its magnetic behavior. In order to clarify the situation, we carried out density functional theory (DFT) calculations using the WIEN2k code[17] and the on-site PBE0 hybrid functional.[18] Our results show that the magnetic structure (i.e., ferrimagnetism originating from the antiparallel coupling of the two Fe^{3+} octahedral and tetrahedral sublattices) described in the space group $Ia\bar{3}d$ is more favorable than the one described in the space group $R\bar{3}$, by about 480 meV per formula units.

$Y_3Fe_5O_{12}$ materials were prepared via conventional high-temperature solid-state reactions, and the purity of the samples was checked by X-ray diffraction. All patterns were refined with the cubic structure (JCPDS No. 83-1027), reflecting that the compounds are single-phased. Rietveld refinement were carried out on undoped YIG (Figure 1), and the refined lattice parameter was determined to be equal to 12.3736(5) Å at room temperature, in good agreement with the literature.[19,20]

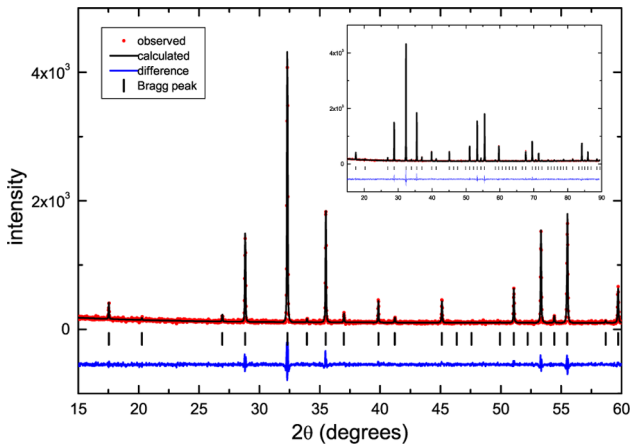

Figure 1. Rietveld refinement of the powder diffraction data of undoped YIG at room temperature. The space group $Ia\bar{3}d$ was used for the structural model.

The oxidation states of iron cations were checked by ^{57}Fe Mössbauer analyses at room temperature. The spectrum of the undoped yttrium iron garnet is reported in Figure 2. This is a typical spectrum of single-phase YIG.[19,21] The obtained data can be fit with two sextets. The first magnetic sextet (subspectrum 1) corresponds to iron in the octahedral site with an isomer shift δ of 0.378 mm/s, a magnetic hyperfine field B_{Hf} of 49.1 T, and a relative intensity I of 60.5%, while the second sextet (subspectrum 2) corresponds to iron in the tetrahedral site[14,15,19] with δ of 0.146 mm/s, B_{Hf} of 39.7 T, and I of 39.5%. Accounting for Mössbauer analyses, no Fe^{2+} ions are present in the obtained yttrium iron garnet material.

3.2. Optical Properties of $Y_3Fe_5O_{12}$: Effect of the Temperature. Since its discovery in 1956, the optical properties of YIG have been investigated only a few times, mainly by Manning,[22] Wood and Remeika,[23] and Wickersheim and Lefever,[24] on single crystals. Usually, the presence of Fe^{3+} ions in oxides leads to red compounds like in Fe_2O_3, $ZnFe_2O_4$, or $MgFe_2O_4$, for example,[24] but YIG materials exhibit a

dx.doi.org/10.1021/ic501708b | Inorg. Chem. 2014, 53, 12378−12383

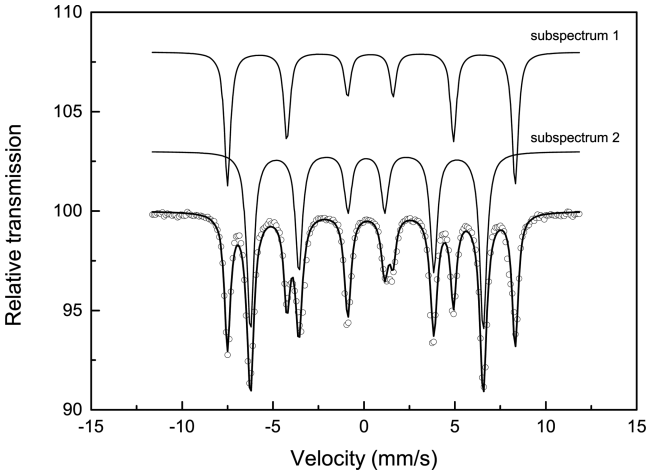

Figure 2. Mössbauer spectrum of $Y_3Fe_5O_{12}$. Experimental data are represented with open circles, and calculated spectrum is represented with black line. The subspectra 1 and 2 correspond to the octahedral site (δ = 0.378 mm/s, B_{Hf} = 49.1 T, I = 60.5%) and the tetrahedral site (δ = 0.156 mm/s, B_{Hf} = 39.7 T, I = 39.5%), respectively.

greenish color. We will thus discuss in more detail the origin of the color in this compound. Before, let us mention that the assignment of absorption spectra of Fe-based compounds may be relatively difficult for at least four reasons: (1) the d−d transitions are parity-forbidden, and consequently, their intensity is expected to be quite weak. However, in many oxides, this rule is not respected because of orbital hybridization and/or spin−orbit coupling. (2) These d−d bands often overlap the charge transfer edge, specially for Fe^{3+} ions. (3) Fe^{3+} and Fe^{2+} often coexist, and their d−d bands are localized in the same wavelength range. (4) The simultaneous presence of Fe^{2+} and Fe^{3+} can lead to an intervalency phenomenon.[26] In our compounds, Mössbauer analyses have confirmed the absence of Fe^{2+} ions, and consequently, the color of YIG is originated from the presence of Fe^{3+} only.

Room-temperature optical diffuse reflectance and absorption (i.e., Kubelka−Munk transformed reflectance) spectra of the undoped YIG sample are reported in Figure 3. As already notified in the literature,[22−24,27] the optical properties of YIG originate from the combination of a ligand−metal charge transfer and Fe^{3+} d−d transitions. Thus, the charge transfer from the 2p orbitals of oxygen to the empty 3d orbitals of Fe^{3+} ions[23,24,28] (O^{2-} + Fe^{3+} → O^{-} + Fe^{2+}) is located around 485 nm (2.57 eV) and the d−d transitions range from 1.35 to 2.04 eV. The band assignments can be performed from the Tanabe−Sugano diagram for a d^5 configuration. In the crystal field theory, the splitting of the d-blocks is lesser for a tetrahedral coordination than for the octahedral one. Thus, we can state that the band at 900 nm corresponds to the $^6A_1 \rightarrow {}^4T_1$ transition of iron ions in the octahedral site.[22−24,27] Furthermore, the bands located around 600 nm and the shoulder at 700 nm can be assigned to the $^6A_1 \rightarrow {}^4T_2$ transition of Fe^{3+} ions in the octahedral site with a contribution of $^6A_1 \rightarrow {}^4T_1$, $^4T_2$ transitions of Fe^{3+} ions in the tetrahedral site. Nevertheless, a potential contribution of the $^6A_1 \rightarrow {}^4A_1,{}^4E_1$ transitions in this visible domain cannot be fully ruled out even if expected at higher energy.

According to the optical measurements, the greenish color of YIG compounds is originated from the slight absorption in the violet range (charge transfer) as well as the presence of d−d transitions in the orange-red region. Consequently, based on our previous postulate, a temperature increase should cause a charge transfer shift correlated with the thermal expansion of the unit cell and an increase of metal−oxygen interatomic distances. If the charge transfer shift is large enough, the YIG color can be modified. Namely, the ligand-to-metal charge transfer absorption may overlap progressively on the green region of the visible spectrum leading to a greenish-reddish transition, if d−d transitions do not shift in energy with temperature.[11]

The thermochromism of undoped YIG was investigated and followed by diffuse reflectance spectroscopy from room temperature to 300 °C (Figure 3). The continuous red shift of the absorption edge is observed with temperature, whereas the positioning of d−d absorption bands is only very weakly affected. This regular shift goes along with a slight elongation of ionic bonds with temperature, which is evidenced by an increase of the lattice parameters (Figure 4). The expansion implies a reduction of the electrostatic interaction of the d electrons, resulting in a lowering of the position of the d^6 energy level of Fe^{2+}. Consequently the O^{2-} → Fe^{3+} charge

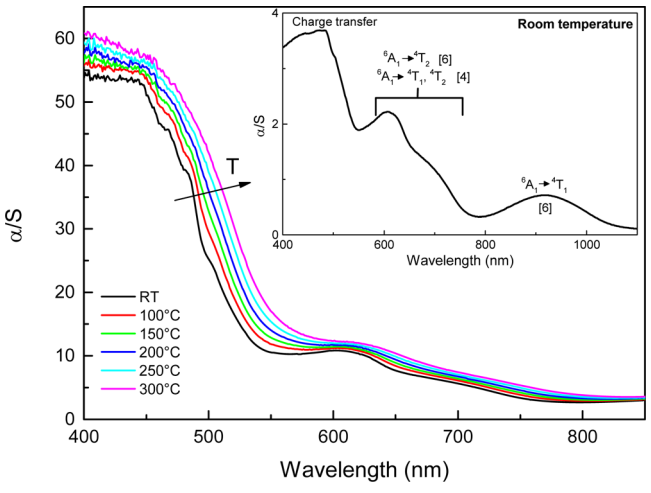

Figure 3. Kubelka−Munk transformed reflectivity vs wavelength of undoped $Y_3Fe_5O_{12}$ at room temperature (inset) and for different temperature.

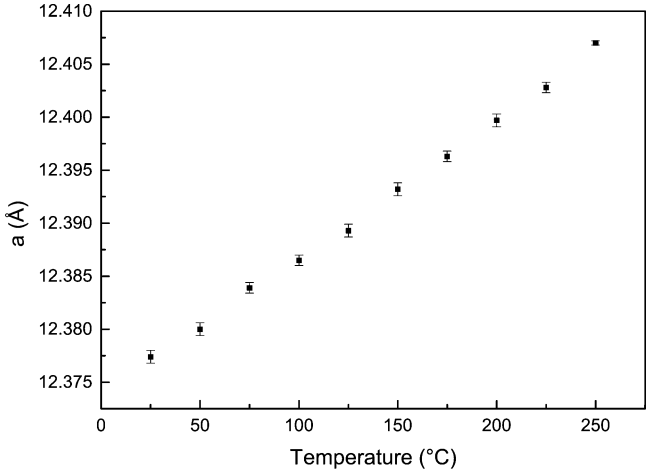

Figure 4. Evolution of refined lattice parameters of $Y_3Fe_5O_{12}$ with temperature.

dx.doi.org/10.1021/ic501708b | Inorg. Chem. 2014, 53, 12378−12383

transfer occurs at lower energy. The continuous red shift is estimated around 0.05 eV/100 °C, which is quite low compared to the usual shift (0.1 eV/100 °C[25]) observed in semiconductors such as ZnO, Bi_2O_3, ... In order to investigate this aspect from first-principles calculations, we have used three models considering the magnetic structure described in the space group $Ia\bar{3}d$ with increasing the a parameter of the cubic unit cell, i.e., $[a + 0]$, $[a + 0.1]$, and $[a + 0.2]$ Å, respectively. We found a linear relationship between the charge transfer band position and the cell parameters showing a red shift of −0.05 eV/0.1 Å. Although this theoretical shift is too small compared to experiments, it provides a qualitative confirmation that the volume expansion leads to a red shift of the charge transfer optical transitions. To illustrate the impact of the red shift on the color rendering, pictures were taken for different temperatures and are reported in Figure 5 with CIE-Lab

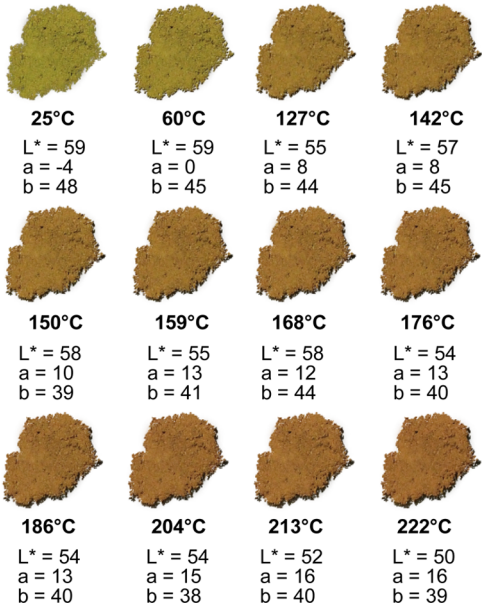

Figure 5. Photographs of undoped YIG at different temperatures and CIELAB parameters (the temperature measurements have been carried out with an optical pyrometer).

parameters. Thus, it appears clear by the naked eye that the evolution of the charge transfer with the temperature leads to a color change in the [20−150 °C] range as asserted by the examination of the L^*ab parameters. Beyond 150 °C, no significant modification of the chromatic coefficient is observed.

The originality of the YIG compound lies in the association of a charge transfer located in the violet range with d−d transitions in the visible region, which leads to a greenish initial color that is impossible to obtain with only a charge transfer. Furthermore, the color change with temperature is due to the presence of charge transfer only (abrupt threshold moving from 2.52 to 2.39 eV) and not to the d−d transitions whose position does not change with temperature. Thus, in this study, instead of combining a semiconductor and a d−d transition based-compound to obtain a new inorganic thermochromic material, we have an original material where the mixing rule occurs[11] directly within the same single-phase material.

4. OPTICAL PROPERTIES OF CR-DOPED $Y_3FE_5O_{12}$

Although the thermochromic behavior of YIG might be considered for temperature indicator applications, the color at low and high temperature still remains not saturated. The chromatic coefficient can certainly be tuned via a control of the grain size to favor scattering, but no effect on the YIG color was observed when grain size was reduced by ball-milling. The YIG host lattice can also be easily doped with various ions,[14,15,20,23,29,30] and consequently, attempts to dope the host lattice with several guest ions (e.g., Al^{3+}, Ga^{3+}, Mn^{2+}, ...) were envisioned. Unfortunately, only chromium ions turn out to have an impact on the colors of the parent host lattice.

Chromium-doped $Y_3Fe_5O_{12}$ compounds were prepared with substitution of Cr for Fe up to 10 mol %, and the purity of all doped samples was checked by X-ray diffraction. In Figure 6 is

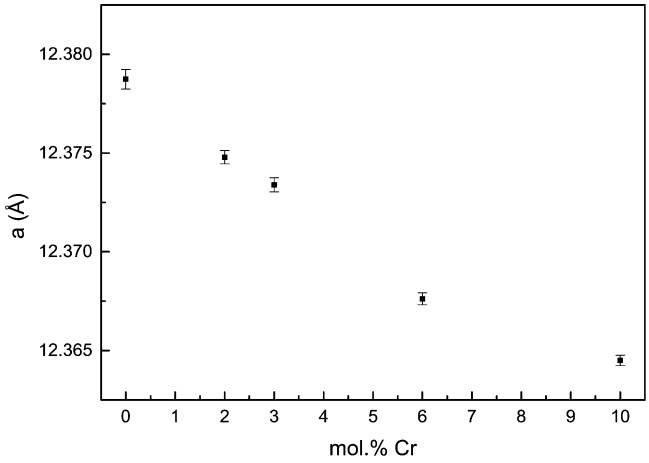

Figure 6. Variation of the lattice parameters of $Y_3Fe_5O_{12}$:x% Cr with the molar percentage of chromium.

depicted the variation of the lattice parameters with the chromium content. The decrease in the unit cell volume with Cr percentage can be attributed to the smaller ionic radius of 6-fold high spin Cr^{3+} (0.61 Å) compared to that of 6-fold high spin Fe^{3+} (0.64 Å).[31] This result is in good agreement with the literature where the preference of Cr^{3+} for the octahedral site was proved, especially from Mössbauer measurements.[14,20,30]

The introduction of chromium cations in the YIG structure leads to a clear color change at room temperature of the material from greenish to brownish (Figure 7). This color change is very similar to that induced by a temperature increase in YIG, although the chromium doping induces a contraction of the lattice contrary to the effect of a temperature increase. The optical properties of doped compounds have been also investigated by diffuse reflectance and compared with the undoped sample. Clearly, the substitution of chromium for iron causes a visible red shift of the charge transfer, mainly responsible for the color change, and a reinforcement of the d−d transitions located at around 700 nm, the others being affected neither in intensity nor in position. The impact of chromium addition on the charge transfer red shift can be explained in two ways: (1) the Cr^{3+} may be at the origin of an inductive effect on the Fe−O bonds and, consequently, on the $O^{2-} \rightarrow Fe^{3+}$ charge transfer[32,33] or (2) the Cr^{3+} may have a direct contribution on the absorption spectrum with the generation of a specific $O^{2-} \rightarrow Cr^{3+}$ charge transfer.

In the former case, the red shift can be explained by an inductive effect that should occur with the introduction of chromium ions in the host lattice. If we consider the purely ionic model of Brown and Altermatt[34] to estimate bond valence, we may assume that the substitution replacement of

dx.doi.org/10.1021/ic501708b | Inorg. Chem. 2014, 53, 12378−12383

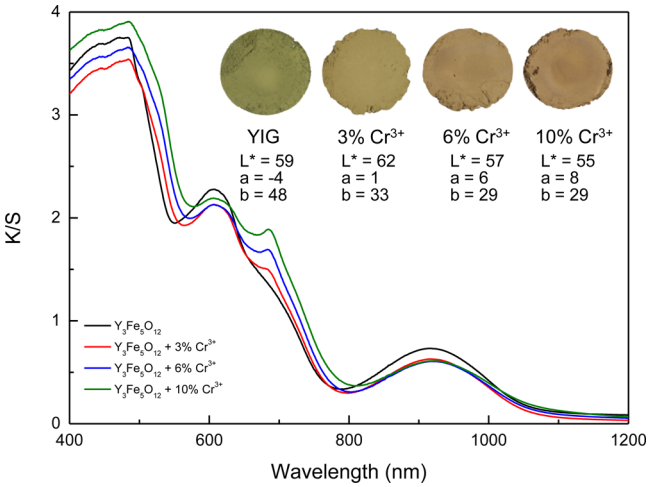

Figure 7. Room-temperature α/S spectrum (Kubelka–Munk transformation) of undoped YIG and Cr^{3+}-doped YIG, with photographs and CIE-Lab parameters.

Fe^{3+} by Cr^{3+} in one octahedron goes along with an adjustment of bond distances around this octahedron to maintain the ionic bond valence of each ion. Actually, the substitution of chromium for iron ion in a regular FeO_6 octahedron (without any change of metal–oxygen bond lengths) leads to a calculated valence of +2.70 for Cr against +3.00 for Fe, i.e., a 10% difference. To counterbalance the valence deviation, metal–oxygen bonds in the substituted octahedron will need to be reduced, which will impact the metal–oxygen bonds (and especially the Fe–O bonds) in the surrounding. Thus, the introduction of many chromium ions would create an expansion effect of the O–Fe bonds in the vicinity of the $[CrO_6]$ octahedron to maintain the ideal valence for all ions, which could explain the red shift and simulate the effect of temperature in undoped $Y_3Fe_5O_{12}$.

In the latter case, the red shift going from undoped $Y_3Fe_5O_{12}$ to Cr^{3+}-doped $Y_3Fe_5O_{12}$ would be correlated to the appearance of new accessible electronic states within the forbidden gap that may play a major role in absorption phenomena. Actually, the band structure of the YIG can be viewed as built upon a valence band consisting mainly of O-2p orbitals and a conduction band consisting of Y-4d orbitals. The Fe-3d levels are located between the VB and the CB (Figure 8) and give rise to absorptions at energy lower than 2.04 eV (d–d transitions), as explained previously (see inset in Figure 8). Charge transfer from oxygen toward iron takes place at higher energy (about 2.4 eV) and is associated with the oxidation of O^{2-} anions into O^- ones concomitantly with the reduction of Fe^{3+} cations into Fe^{2+} ones, O^- and Fe^{2+} being photogenerated metastable species that recombined instantaneously. Because of strong Coulomb repulsions related to the pairing of two electrons in the same orbital, the $3d^6$ configuration of Fe^{2+} cations is expected at much higher energy than the $3d^5$ configuration of Fe^{3+} cations, naturally strongly stabilized due to its half-filled subshell. When Cr^{3+} cations substitute Fe^{3+} ones, extra intrasite d–d transitions occur, which may explain the appearance of absorption shoulders and intensity changes in the low energy part of the absorption spectrum (Figure 7). However, the Cr^{3+} d–d transitions overlap with those of Fe^{3+} and do not modify the hue. In contrast, chromium strongly influences the positioning in energy of the charge transfer. Indeed, the $O^{2-} \rightarrow Cr^{3+}$ charge transfer is expected to take place at a lower energy than the $O^{2-} \rightarrow Fe^{3+}$ one because the $3d^4$ high spin electronic configuration of Cr^{2+} ions is expected to lie below the $3d^6$ high spin configuration of Fe^{2+} cations.[35] Consequently, the Cr^{3+}/Fe^{3+} substitution simulates a temperature increase: the higher the substitution rate, the more red-shifted the charge transfer.

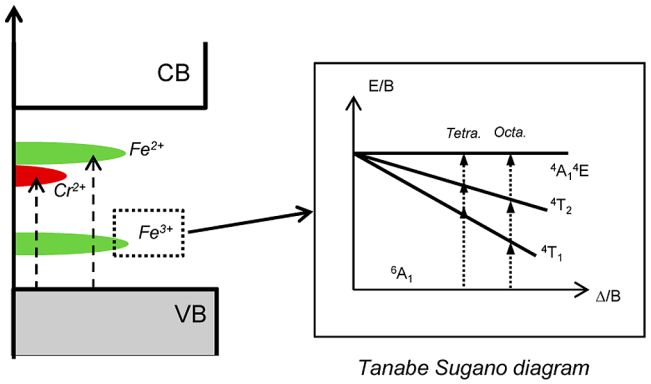

Figure 8. Schematic band structure of YIG when doped with chromium ions and Tanabe–Sugano diagram for the d^5 configuration (inset).

5. CONCLUSION

In this work, we have reported for the first time the reversible thermochromic behavior of the yttrium iron garnet. The intrinsic optical properties of YIG are originated from O^{2-}–Fe^{3+} ligand-to-metal charge transfer together with d–d transitions of Fe^{3+} ions in octahedral and tetrahedral configurations. By increasing the temperature, the color changes continuously from a greenish to a brownish tone due to a regular red shift of the absorption threshold associated with the ionic bond dilatation.

The chromium doping tends to simulate the effect of a temperature increase with regular red shift when raising the Cr^{3+} content. The role of Cr^{3+} is explained by a modification of the electronic structure and the apparition of an $O^{2-} \rightarrow Cr^{3+}$ charge transfer at lower energy than that of O^{2-}–Fe^{3+}.

AUTHOR INFORMATION

Corresponding Authors

*E-mail: helene.brault@cnrs-imn.fr. Fax: (+33)240-373-995 (H.S.-B.).

*E-mail: stephane.jobic@cnrs-imn.fr (S.J.).

Notes

The authors declare no competing financial interest.

REFERENCES

(1) Nassau, K. *The Physics and Chemistry of Color*; John Wiley & Sons: New York, 1983.

(2) Sone, K.; Fukada, Y. *Inorganic Thermochromism*; Springer-Verlag: Berlin, 1923.

(3) Robertson, L.; Gaudon, M.; Pechev, S.; Demourgues, A. *J. Mater. Chem.* **2012**, *22*, 3585–3590.

(4) Eom, S. H.; Kim, D. J.; Yu, Y.-M.; Choi, Y. D. *J. Alloys Compd.* **2005**, *388*, 190–194.

(5) Gaudon, M.; Carbonera, C.; Thiry, A. E.; Demourgues, A.; Deniard, P.; Payen, C.; Letard, J.-F.; Jobic, S. *Inorg. Chem.* **2007**, *46*, 10200–10207.

(6) Kiri, P.; Hyett, G.; Binions, R. *Adv. Mater. Lett.* **2010**, *1*, 86–105.

(7) Robertson, L. C.; Gaudon, M.; Jobic, S.; Deniard, P.; Demourgues, A. *Inorg. Chem.* **2011**, *50*, 2878–2884.

(8) Thiry, A.-E.; Gaudon, M.; Payen, C.; Daro, N.; Letard, J.-F.; Gorsse, S.; Deniard, P.; Rocquefelte, X.; Demourgues, A.; Whangbo, M.-H.; Jobic, S. *Chem. Mater.* **2008**, *20*, 2075−2077.
(9) Gaudon, M.; Deniard, P.; Demourgues, A.; Thiry, A.-E.; Carbonera, C.; Le Nestour, A.; Largeteau, A.; Letard, J.-F.; Jobic, S. *Adv. Mater. (Weinheim, Ger.)* **2007**, *19*, 3517−3519.
(10) Zhang, Z.; Gao, Y.; Luo, H.; Kang, L.; Chen, Z.; Du, J.; Kanehira, M.; Zhang, Y.; Wang, Z. L. *Energy Environ. Sci.* **2011**, *4*, 4290−4297.
(11) Gaudon, M.; Deniard, P.; Voisin, L.; Lacombe, G.; Darnat, F.; Demourgues, A.; Perillon, J.-L.; Jobic, S. *Dyes Pigm.* **2012**, *95*, 344−350.
(12) Petricek, V.; Dusek, M.; Palatinus, L. *JANA2006: Crystallographic Computing System*; Institute of Physics: Prague, Czech Republic, 2006.
(13) Berar, J.-F.; Lelann, P. *J. Appl. Crystallogr.* **1991**, *24*, 1−5.
(14) Bouziane, K.; Yousif, A.; Widatallah, H. M.; Amighian, J. *J. Magn. Magn. Mater.* **2008**, *320*, 2330−2334.
(15) Cheng, Z.; Cui, Y.; Yang, H.; Chen, Y. *J. Nanopart. Res.* **2009**, *11*, 1185−1192.
(16) Rodic, D.; Mitric, M.; Tellgren, R.; Rundlof, H.; Kremenovic, A. *J. Magn. Magn. Mater.* **1999**, *191*, 137−145.
(17) Blaha, P.; Schwarz, K.; Kvasnicka, D.; Luitz, J. *WIEN2k: An Augmented Plane Wave+LO Program for Calculating Crystal Properties*; Techn. Universität Wien.: Vienna, 2001.
(18) Perdew, J. P.; Ernzerhof, M.; Burke, K. *J. Chem. Phys.* **1996**, *105*, 9982−9985.
(19) Garskaite, E.; Gibson, K.; Leleckaite, A.; Glaser, J.; Niznansky, D.; Kareiva, A.; Meyer, H.-J. *Chem. Phys.* **2006**, *323*, 204−210.
(20) Murumkar, V. D.; Modi, K. B.; Jadhav, K. M.; Bichile, G. K.; Kulkarni, R. G. *Mater. Lett.* **1997**, *32*, 281−285.
(21) Waerenborgh, J. C.; Rojas, D. P.; Shaula, A. L.; Kharton, V. V.; Marques, F. M. B. *Mater. Lett.* **2004**, *58*, 3432−3436.
(22) Manning, P. G. *Can. Mineral.* **1972**, *11*, 826−839.
(23) Wood, D. L.; Remeika, J. P. *J. Appl. Phys.* **1967**, *38*, 1038−1045.
(24) Wickersheim, K. A.; Lefever, R. A. *J. Chem. Phys.* **1962**, *36*, 844−850.
(25) Pailhe, N.; Wattiaux, A.; Gaudon, M.; Demourgues, A. *J. Solid State Chem.* **2008**, *181*, 1040−1047.
(26) Marfunin, A. S. *Physics of Minerals and Inorganic Materials*; Springer-Verlag: Berlin, 1979.
(27) Wemple, S. H.; Blank, S. L.; Seman, J. A.; Biolsi, W. A. *Phys. Rev. B: Solid State* **1974**, *9*, 2134−2144.
(28) Grant, P. M.; Ruppel, W. *Solid State Commun.* **1967**, *5*, 543−546.
(29) Naik, S. R.; Salker, A. V. *Phys. Chem. Chem. Phys.* **2012**, *14*, 10032−10040.
(30) Kuznetsov, M. V.; Pankhurst, Q. A.; Parkin, I. P.; Affleck, L.; Morozov, Y. G. *J. Mater. Chem.* **2000**, *10*, 755−760.
(31) Shannon, R. D.; Prewitt, C. T. *Acta Crystallogr., Sect. B* **1969**, *25*, 925−946.
(32) Etourneau, J.; Portier, J.; Menil, F. *J. Alloys Compd.* **1992**, *188*, 1−7.
(33) Gauthier, G.; Jobic, S.; Boucher, F.; Macaudiere, P.; Huguenin, D.; Rouxel, J.; Brec, R. *Chem. Mater.* **1998**, *10*, 2341−2347.
(34) Brown, I. D.; Altermatt, D. *Acta Crystallogr., Sect. B* **1985**, *B41*, 244−247.
(35) Orofino, H.; Machado, S. P.; Faria, R. B. *Quim. Nova* **2013**, *36*, 894−896.